

# Tight finite-resource bounds for private communication over Gaussian channels

Riccardo Laurenza,<sup>1,2</sup> Spyros Tserkis,<sup>3</sup> Leonardo Banchi,<sup>4</sup> Samuel L. Braunstein,<sup>1</sup> Timothy C. Ralph,<sup>3</sup> and Stefano Pirandola<sup>1,5</sup>

<sup>1</sup>*Computer Science and York Centre for Quantum Technologies, University of York, York YO10 5GH, United Kingdom*

<sup>2</sup>*QSTAR, INO-CNR and LENS, Largo Enrico Fermi 2, 50125 Firenze, Italy*

<sup>3</sup>*Centre for Quantum Computation and Communication Technology,*

*School of Mathematics and Physics, University of Queensland, St Lucia, Queensland 4072, Australia*

<sup>4</sup>*Department of Physics and Astronomy, University of Florence,  
via G. Sansone 1, I-50019 Sesto Fiorentino (FI), Italy*

<sup>5</sup>*Research Laboratory of Electronics, Massachusetts Institute of Technology (MIT), Cambridge, Massachusetts 02139, USA*

Upper bounds for private communication over quantum channels can be computed by adopting channel simulation, protocol stretching, and relative entropy of entanglement. All these ingredients have led to single-letter upper bounds to the secret key capacity which are easily computed over suitable resource states. For bosonic Gaussian channels, the tightest upper bounds have been derived by considering teleportation simulation and asymptotic resource states, namely the asymptotic Choi matrices of the Gaussian channels. These states are generated by propagating part of a two-mode squeezed vacuum state through the channel and then taking the limit of infinite energy. So far, it has been an open problem to find alternative finite-energy resource states so that the teleportation simulation would imply a close approximation of the infinite-energy upper bounds. In this work we show this is indeed possible. We show how a class of finite-energy resource states are able to increasingly approximate the infinite-energy bounds for decreasing purity, so that they provide tight upper bounds to the secret-key capacity of one-mode phase-insensitive Gaussian channels.

## I. INTRODUCTION

The ultimate performance of a communication channel is given by its capacity. In quantum information theory [1–4], there are several definitions of capacity, depending on whether one wants to send classical information, quantum information, entanglement etc. In particular, the secret-key capacity of a quantum channel represents the maximum number of secret bits that two authenticated remote users may extract at the ends of the channel, without any restrictions on their local operations (LOs) and classical communication (CC), briefly called LOCCs. This capacity is particularly important because it upper-bounds the secret key rate of any point-to-point protocol of quantum key distribution (QKD) [5–7]. In this context, the highest key rates are those achievable by QKD protocols implemented with continuous-variable (CV) systems, i.e., bosonic modes of the electromagnetic field, which are conveniently prepared in Gaussian states [8–12]. These quantum states are transmitted through optical fibers or free-space links which are typically modeled as one-mode Gaussian channels [13].

Exploring the ultimate achievable rates of CV-QKD [14–22] has been a very active research area. Back in 2009, a lower bound to the secret key capacity of the thermal-loss channel was given [23] in terms of the reverse coherent information [24, 25]. In 2014, the first (non-tight) upper bound was found by resorting to the squashed entanglement [26]. More recently, a tighter upper bound has been established by Ref. [27] in terms of the relative entropy of entanglement (REE) [28, 29]. For a pure-loss channel, the lower and upper bounds of Refs. [23, 27] coincide so that the secret-key capacity of this channel is fully established. This is also known as the PLOB bound [27] and fully characterizes the rate-loss scaling which affects any point-to-point QKD protocol.

One of the main tools used in Ref. [27] was channel simulation, where a quantum channel is simulated by applying an

LOCC to a suitable resource state. In particular, for the so-called teleportation covariant channels, this simulation corresponds to teleporting [30] over the Choi matrix of the channel, a property first noted for Pauli channels [31, 32]. Using this tool, one can replace each transmission through a quantum channel with its simulation and re-organize an adaptive (feedback-assisted) QKD protocol over the channel into a much simpler block version. This technique is also known as teleportation stretching and its combination with an entanglement measure as the REE allows one to write simple single-letter upper bounds for the secret-key capacity [27].

This methodology can be applied to bosonic Gaussian channels. In particular, since these channels are teleportation-covariant, they can be simulated by applying the CV teleportation protocol [33–38] over their asymptotic Choi matrices, as discussed in Refs. [27, 39, 40]. A bosonic Choi matrix is defined by propagating part of a two-mode squeezed vacuum (TMSV) state [8] through the channel, and taking the limit of infinite energy. Therefore, the Choi matrix of a bosonic channel is more precisely a limit over a succession of states. This also means that a finite-energy simulation of a Gaussian channel, performed by teleporting over a TMSV state, turns out to be imperfect with an associated simulation error which must be carefully handled and propagated to the output of adaptive protocols [27, 41].

An alternative way to simulate Gaussian channels is to implement the CV teleportation protocol over a suitably-defined class of finite-energy Gaussian states. This approach removes the limit of infinite energy in the resource state, even though it still utilizes CV Bell detection, which is defined as an asymptotic Gaussian measurement, whose limit realizes an ideal projection onto displaced Einstein-Podolsky-Rosen (EPR) states. As shown in Ref. [42–44], it is possible to realize such a finite-resource simulation. However, by combining this type of channel simulation with the ingredients of Ref. [27], i.e., teleportation stretching and REE, one is not

able to closely approximate the upper bounds to the secret key capacity of bosonic Gaussian channels. This was shown in Ref. [45] for the various phase-insensitive Gaussian channels. Finite-resource simulation for the specific case of the thermal-loss channel and assuming a finite number of channel uses has also been considered in Ref. [46]. More specifically, adopting teleportation stretching [27, 41] and simulating the channel by numerically produced appropriate resource states, the authors in Ref. [46] showed that REE can approximate the upper bound to the secret key capacity established by PLOB for the thermal-loss channel [27].

More recently, in Ref. [47] all possible resource states able to simulate a given Gaussian channel through teleportation with finite resources were found analytically, and their performance in terms of the entanglement of formation was studied. In this work, we adopt this class of states, which can be parametrized in terms of their purity and they are optimized with respect to the REE. Following the tools of Ref. [27], we therefore derive corresponding upper bounds to the secret-key capacity of bosonic Gaussian channels. Remarkably, these finite-energy upper bounds can be made as close as possible to the infinite-energy bounds of Ref. [27] for all the phase-insensitive Gaussian channels, in particular, thermal-loss channels, pure-loss channels, amplifiers, quantum-limited amplifiers, and additive-noise Gaussian channels.

The paper is organized as follows. In Sec. II, we provide some preliminaries on Gaussian states, Gaussian channels, and the quantification of entanglement via the REE. In Sec. III, we discuss the teleportation simulation of Gaussian channels based on the new class of resource states. In Sec. IV we apply this tool to bound the secret-key capacity of the phase-insensitive Gaussian channel, showing how our finite-energy bounds are able to closely approximate the infinite-energy bounds. Sec. V is for conclusions.

## II. PRELIMINARIES

### A. Gaussian states

Any quantum  $n$ -mode bosonic state  $\hat{\sigma}$  can be described by a vector of quadrature field operators  $\hat{q} := (\hat{x}_1, \hat{p}_1, \dots, \hat{x}_n, \hat{p}_n)^T$ , with  $\hat{x}_j := \hat{a}_j + \hat{a}_j^\dagger$  and  $\hat{p}_j := i(\hat{a}_j^\dagger - \hat{a}_j)$ , where  $\hat{a}_j$  and  $\hat{a}_j^\dagger$  are the annihilation and creation operators, respectively, with commutator  $[\hat{a}_i, \hat{a}_j^\dagger] = \delta_{ij}$ . Bosonic Gaussian states are those states which can be fully characterized by the mean value and covariances between the quadratures  $\hat{q}$ .

For simplicity, a two-mode Gaussian state (assuming without losing generality zero mean value) can be fully described by a real and positive-definite matrix called the covariance matrix (CM), i.e.,  $\sigma_{ij} = \frac{1}{2} \langle \{\hat{q}_i, \hat{q}_j\} \rangle$ , where  $\{, \}$  is the anti-commutator [8, 9, 11]. In the standard form  $\sigma$  is given by

[48, 49]

$$\sigma^{\text{sf}} = \begin{bmatrix} a & 0 & c_1 & 0 \\ 0 & a & 0 & c_2 \\ c_1 & 0 & b & 0 \\ 0 & c_2 & 0 & b \end{bmatrix}. \quad (1)$$

Using symplectic transformations,  $S$ , any two-mode CM can be transformed into  $\nu = S\sigma S^T = \nu_- \mathbb{1} \oplus \nu_+ \mathbb{1}$ , where  $1 \leq \nu_- \leq \nu_+$  are called symplectic eigenvalues [8, 50]. The purity of the state is given by  $\mu = (\nu_- \nu_+)^{-1}$ .

### B. Gaussian channels

Decoherence of quantum states is modeled through quantum channels which are described by a completely positive trace-preserving map  $\mathcal{C}$  [8, 11, 51]. Consider a two-mode (zero-mean) Gaussian state with CM  $\sigma_{\text{in}}$ . Assume that the second mode is processed by a single-mode Gaussian channel  $\mathcal{G}$ . Then, we have the following input-output transformation for the CM

$$\sigma_{\text{in}} \xrightarrow{\mathcal{G}} \sigma_{\text{out}} = (\mathbb{1} \oplus \mathcal{U})\sigma_{\text{in}}(\mathbb{1} \oplus \mathcal{U})^T + (0 \oplus \mathcal{V}), \quad (2)$$

where  $\mathcal{U} = \sqrt{\tau} \mathbb{1}$  represents the attenuation/amplification operation and  $\mathcal{V} = v \mathbb{1}$  the induced noise. Phase-insensitive Gaussian channels are the following [8, 51–53]: (i) the loss channel  $\mathcal{L}$  with transmissivity  $0 < \tau < 1$  and noise  $v = |1 - \tau|(2\bar{n} + 1)$ , where  $\bar{n}$  indicates the mean number of photons of the environment (pure-loss channel or quantum-limited attenuator for  $\bar{n} = 0$ ), (ii) the amplifier channel  $\mathcal{A}$  with gain  $\tau > 1$  and noise  $v = |1 - \tau|(2\bar{n} + 1)$  (pure amplifier or quantum-limited amplifier for  $\bar{n} = 0$ ), (iii) the additive-noise Gaussian channel  $\mathcal{N}$  with  $\tau = 1$  and added-noise variance  $v > 0$ , and (iv) the identity channel  $\mathcal{I}$  with  $\tau = 1$  and  $v = 0$ , representing the ideal non-decohering channel. Note that we do not consider the conjugate of the amplifier channel because it is entanglement-breaking and, therefore, has zero secret-key capacity.

### C. Quantification of entanglement

The *bona fide* measure of entanglement for pure states is the entropy of entanglement [31], defined as  $\mathcal{E}(\hat{\rho}) := S(\text{tr}_B \hat{\rho})$ , where  $S(x) := -\text{tr}(x \log_2 x)$  is the von Neumann entropy, and  $\text{tr}_B$  denotes the partial trace over subsystem  $B$  [54]. For mixed states several measures have been defined in the literature with different operational meanings [55–58]. In this work we use the REE [28, 29] defined by

$$\mathcal{E}_R(\hat{\rho}) := \inf_{\hat{\rho}_{\text{sep}}} S(\hat{\rho} || \hat{\rho}_{\text{sep}}), \quad (3)$$

where  $\hat{\rho}_{\text{sep}}$  is an arbitrary separable state and

$$S(\hat{\rho} || \hat{\rho}_{\text{sep}}) := \text{tr}[\hat{\rho}(\log_2 \hat{\rho} - \log_2 \hat{\rho}_{\text{sep}})] \quad (4)$$

is the relative entropy.

The REE is a direct generalization of the von Neumann mutual information and has a geometrical interpretation, since it quantifies the distance between an entangled state and its closest separable state. In general the computation of REE is a challenging task, and thus we can calculate it only numerically. However, for Gaussian states an upper bound of it can be defined by fixing a candidate separable state [27]. Specifically, for a Gaussian state  $\hat{\rho}$  with CM  $\rho$  of the form of Eq. (1), we pick a separable state  $\hat{\rho}_{\text{sep}}^*$  that has CM  $\rho_{\text{sep}}^*$ , with the same diagonal blocks as  $\rho$ , but where the off-diagonal terms are replaced as follows

$$c_{1,2} \rightarrow \pm \sqrt{(a-1)(b-1)}. \quad (5)$$

Using the separable state  $\hat{\rho}_{\text{sep}}^*$  we can then write the upper bound

$$\mathcal{E}_R(\hat{\rho}) \leq \mathcal{E}_R^*(\hat{\rho}) := \mathcal{S}(\hat{\rho} || \hat{\rho}_{\text{sep}}^*). \quad (6)$$

The distance  $\mathcal{S}(\hat{\rho} || \hat{\rho}_{\text{sep}}^*)$  can be calculated using the closed analytical formula derived in Ref. [27], which is reviewed (and extended) in Appendix A and is based on the Gibbs representation for Gaussian states [59]. More precisely, for two zero-mean Gaussian states with CMs  $\rho_k$  and  $\rho_\ell$ , their relative entropy is given by

$$\mathcal{S}(\hat{\rho}_k || \hat{\rho}_\ell) = \Sigma(\rho_k, \rho_\ell) - \Sigma(\rho_k, \rho_k), \quad (7)$$

where we have defined

$$\Sigma(\rho_k, \rho_\ell) := \frac{\ln \det \left( \frac{\rho_\ell + i\Omega}{2} \right) + \text{tr} \left( \frac{\rho_k \mathbf{G}_\ell}{2} \right)}{2 \ln 2}, \quad (8)$$

with  $\mathbf{G}_k = 2i\Omega \coth^{-1}(i\rho_k \Omega)$  [59], and the matrix  $\Omega = \omega \oplus \omega$  is the symplectic form, with  $\omega = \begin{bmatrix} 0 & 1 \\ -1 & 0 \end{bmatrix}$ .

### III. FINITE-RESOURCE TELEPORTATION SIMULATION

As discussed in Ref. [27], an arbitrary channel  $\mathcal{C}$  is called LOCC-simulable or  $\hat{\rho}$ -stretchable if it can be simulated by a trace-preserving LOCC,  $\Lambda$ , and a suitable resource state  $\hat{\rho}$ , i.e.

$$\mathcal{C}(\hat{\sigma}) = \Lambda(\hat{\sigma} \otimes \hat{\rho}). \quad (9)$$

An important class is that of the Choi-stretchable channels, which can be simulated via the Choi-state, defined as  $\hat{\rho}^{\text{Choi}} := \mathcal{I} \otimes \mathcal{C}(\hat{\varphi})$ , with  $\hat{\varphi}$  being the maximally entangled state. This is always possible if  $\mathcal{C}$  is teleportation-covariant, i.e., it is covariant with respect to the random unitaries of teleportation [27]. In that case, the resource state is its Choi matrix  $\hat{\rho}^{\text{Choi}}$  and the LOCC  $\Lambda$  is teleportation.

As already mentioned before, bosonic Gaussian channels  $\mathcal{G}$  are teleportation-covariant, but their Choi matrices are asymptotic states. One starts by considering a TMSV state  $\hat{\varphi}_\omega$  with variance  $\omega = 2\bar{n} + 1$ , with  $\bar{n}$  being the mean number of photons in each local mode. This is then partly propagated through  $\mathcal{G}$  so as to define its quasi-Choi matrix  $\hat{\rho}_\omega^{\text{Choi}} :=$

$\mathcal{I} \otimes \mathcal{G}(\hat{\varphi}_\omega)$ . Taking the limit for large  $\omega$ ,  $\hat{\varphi}_\omega$  becomes the ideal EPR state, and  $\hat{\rho}_\omega^{\text{Choi}}$  defines the Choi matrix of  $\mathcal{G}$ . Correspondingly, one may write the following asymptotic simulation for a Gaussian channel

$$\mathcal{G}(\hat{\sigma}) = \lim_{\omega} \Lambda(\hat{\sigma} \otimes \hat{\rho}_\omega^{\text{Choi}}), \quad (10)$$

where  $\Lambda$  is the LOCC associated with CV teleportation [60].

Generalizing previous ideas [42], Ref. [47] has recently shown that an arbitrary single-mode phase-insensitive Gaussian channel  $\mathcal{G} = \mathcal{G}_{\tau,v}$ , with parameters  $\tau$  and  $v$ , can be simulated by CV teleportation  $\Lambda_\tau$  with gain  $\tau$  over a suitable finite-energy resource state  $\hat{\rho}_{\tau,v}$  [47]. In other words, as also depicted in Fig. 1, we may write

$$\mathcal{G}_{\tau,v}(\hat{\sigma}) = \Lambda_\tau(\hat{\sigma} \otimes \hat{\rho}_{\tau,v}), \quad (11)$$

where  $\hat{\rho}_{\tau,v}$  is a zero-mean Gaussian state with CM

$$\rho_{\tau,v} = \begin{bmatrix} a & 0 & c & 0 \\ 0 & a & 0 & -c \\ c & 0 & b & 0 \\ 0 & -c & 0 & b \end{bmatrix}, \quad (12)$$

where the elements of the CM are [47]

$$a = \frac{|1 - \tau|(\nu_+ - \nu_-) + (1 + \tau)v - 2\gamma}{(1 - \tau)^2}, \quad (13)$$

$$b = \frac{\tau|1 - \tau|(\nu_+ - \nu_-) + (1 + \tau)v - 2\gamma}{(1 - \tau)^2}, \quad (14)$$

$$c = \frac{\tau|1 - \tau|(\nu_+ - \nu_-) + 2\tau v - (1 + \tau)\gamma}{\sqrt{\tau}(1 - \tau)^2}, \quad (15)$$

and we have set [61]

$$\gamma := \sqrt{\tau(v - |1 - \tau|\nu_-)(v + |1 - \tau|\nu_+)}. \quad (16)$$

Note that for  $0 < \tau < 1$ , we get states with  $a \geq b$ , while for  $\tau > 1$  we get  $a \leq b$ . These elements are expressed in terms of the channel parameters,  $\tau$  and  $v$ , and may vary over the symplectic spectrum with the constraints

$$1 \leq \nu_- \leq 2\bar{n} + 1, \quad \nu_- \leq \nu_+, \quad (17)$$

where  $\bar{n}$  is the mean thermal number of the Gaussian channel (thermal-loss or amplifier) [62].

According to Eq. (17), for thermal-loss and amplifier channels, we have some freedom in choosing  $\nu_\pm$  so that there is an entire class over which we may optimize our upper bounds. One possible approach is fixing the purity  $\mu = (\nu_- \nu_+)^{-1}$  of the resource state and optimizing over the remaining free parameter. Note that the asymptotic Choi matrix can be retrieved in the limit of  $\mu \rightarrow 0$ . This feature ensures that we can approximate the infinite-energy bounds as much as we want by using a small but yet non-zero value of the purity.

For the special case of  $\tau = 1$ , we have an additive-noise Gaussian channel with added-noise variance  $v > 0$ . In this case, taking the limit  $\tau \rightarrow 1$  for the class in Eqs. (13)-(15) we get the following parametrization

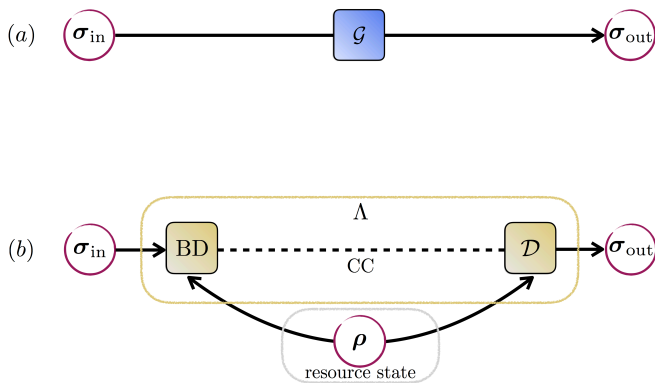


FIG. 1. Finite-resource simulation of Gaussian channels. In panel (a), we depict a phase-insensitive Gaussian channel  $\mathcal{G} = \mathcal{G}_{\tau,v}$  transforming the input state  $\hat{\sigma}_{\text{in}}$  into the output state  $\hat{\sigma}_{\text{out}}$ . In panel (b), we show its teleportation simulation, an LOCC,  $\Lambda$ , over a finite-energy resource state. Its basic components are: a) the local operation (LO), i.e., CV Bell detection (BD) between the input state  $\hat{\sigma}_{\text{in}}$  and the resource state  $\hat{\rho}_{\tau,v}$  of Eqs. (13)-(15); b) the classical communication (CC) of the Bell outcomes; c) a second local operation, i.e., the conditional displacement  $D$  with suitable gain  $\tau$  [34]; d) the output teleported state  $\hat{\sigma}_{\text{out}}$ .

$$a = \frac{\nu_-^2 + 2\nu_-(\nu_+ - v) + (\nu_+ + v)^2}{4v}, \quad (18)$$

$$b = \frac{\nu_-^2 + 2\nu_-(\nu_+ + v) + (\nu_+ - v)^2}{4v}, \quad (19)$$

$$c = \frac{(\nu_- + \nu_+ - v)(\nu_- + \nu_+ + v)}{4v}. \quad (20)$$

#### IV. SECRET-KEY CAPACITY

The most general protocol (graphically depicted in Fig. 2) for key generation is based on adaptive LOCCs. Each transmission through the quantum channel  $\mathcal{C}$  is interleaved between two of such LOCCs. The general formalism can be found in Ref. [27] and goes as follows. Assume that two remote users, Alice and Bob, have two local registers of quantum systems (modes),  $\mathbf{a}$  and  $\mathbf{b}$ , which are in some fundamental state  $\hat{\rho}_{\mathbf{a}} \otimes \hat{\rho}_{\mathbf{b}}$ . The two parties start by applying an adaptive LOCC  $\Lambda_0$  before the first transmission.

In the first use of the channel, Alice picks a mode  $a_1$  from her register  $\mathbf{a}$  and sends it through the channel  $\mathcal{E}$ . Bob gets the output mode  $b_1$  which is included in his local register  $\mathbf{b}$ . The parties apply another adaptive LOCC  $\Lambda_1$ . Then, there is the second transmission and so on. After  $n$  uses, we have a sequence of LOCCs  $\{\Lambda_0, \Lambda_1, \dots, \Lambda_n\}$  characterizing the protocol  $\mathcal{P}$  and an output state  $\hat{\rho}_{\mathbf{ab}}^n$  which is  $\epsilon$ -close to a target private state [63] with  $nR_n$  bits. Taking the limit of large  $n$  and optimizing over the protocols, we define the secret-key capacity of the channel  $\mathcal{C}$  as

$$K(\mathcal{C}) := \sup_{\mathcal{P}} \lim_n R_n. \quad (21)$$

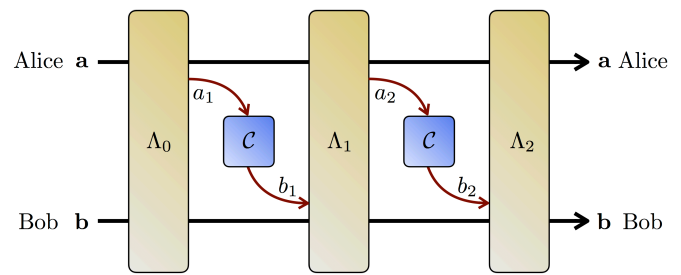


FIG. 2. Schematic description of an adaptive QKD protocol. In the first step, Alice and Bob prepare the initial separable state  $\hat{\rho}_{\mathbf{ab}}$  of their local registers  $\mathbf{a}$  and  $\mathbf{b}$  by applying an adaptive LOCC  $\Lambda_0$ . After the preparation of these registers, there is the first transmission through the quantum channel  $\mathcal{C}$ . Alice picks a quantum system from her local register  $a_1 \in \mathbf{a}$ , which is therefore depleted as  $\mathbf{a} \rightarrow \mathbf{a}a_1$ ; then, system  $a_1$  is sent through the channel  $\mathcal{C}$ , with Bob getting the output  $b_1$ . After transmission, Bob includes the output system  $b_1$  in his local register, which is augmented as  $b_1 \mathbf{b} \rightarrow \mathbf{b}$ . This is followed by Alice and Bob applying another adaptive LOCC  $\Lambda_1$  to their registers  $\mathbf{a}$  and  $\mathbf{b}$ . In the second transmission, Alice picks and sends another system  $a_2 \in \mathbf{a}$  through the quantum channel  $\mathcal{C}$  with output  $b_2$  received by Bob. The remote parties apply another adaptive LOCC  $\Lambda_2$  to their registers and so on. This procedure is repeated  $n$  times, with the output state  $\hat{\rho}_{\mathbf{ab}}^n$  being finally generated for Alice's and Bob's local registers.

Given a phase-insensitive Gaussian channel  $\mathcal{G} = \mathcal{G}_{\tau,v}$  we may write its teleportation simulation by using our resource state  $\hat{\rho} = \hat{\rho}_{\tau,v}$  of Eqs. (13)-(15). Then, we may replace each transmission through the channel by its simulation and stretch the adaptive protocol into a block form [27, 45], so that we may write  $\hat{\rho}_{\mathbf{ab}}^n = \Delta(\hat{\rho}^{\otimes n})$  for a trace-preserving LOCC  $\Delta$ . Finally, we may upper bound the secret-key capacity by computing the REE over the output state  $\hat{\rho}_{\mathbf{ab}}^n$ . Since the REE is monotonic under  $\Delta$  (data processing) and sub-additive over tensor-products, we may write [27, 45]

$$K(\mathcal{G}) \leq \mathcal{E}_R(\hat{\rho}) \leq \mathcal{E}_R^*(\hat{\rho}), \quad (22)$$

where  $\mathcal{E}_R^*$  is defined according to Eq. (6).

In particular, we may fix the purity and compute the upper bound. In other words, let us have a set of resource states  $\hat{\rho} \in \mathcal{R}(\mu)$  expressed by Eqs. (13)-(15), that can simulate the same channel but have different purities  $\mu$ . Then, for any  $\mu$ , we may consider

$$\mathcal{E}_R^*(\hat{\rho}) \leq \mathcal{B}_\mu := \min_{\hat{\rho} \in \mathcal{R}(\mu)} S(\hat{\rho} || \hat{\rho}_{\text{sep}}^*). \quad (23)$$

We know that the minimum value of this bound is reached by the asymptotic Choi matrix of the channel that has vanishing purity. Thus, setting  $\mu \rightarrow 0$  in Eq. (23) we reach a bound equivalent to the infinite energy-bound of [27]

$$\mathcal{B}_0 := \lim_{\mu \rightarrow 0} \mathcal{B}_\mu \leq \mathcal{B}_\mu. \quad (24)$$

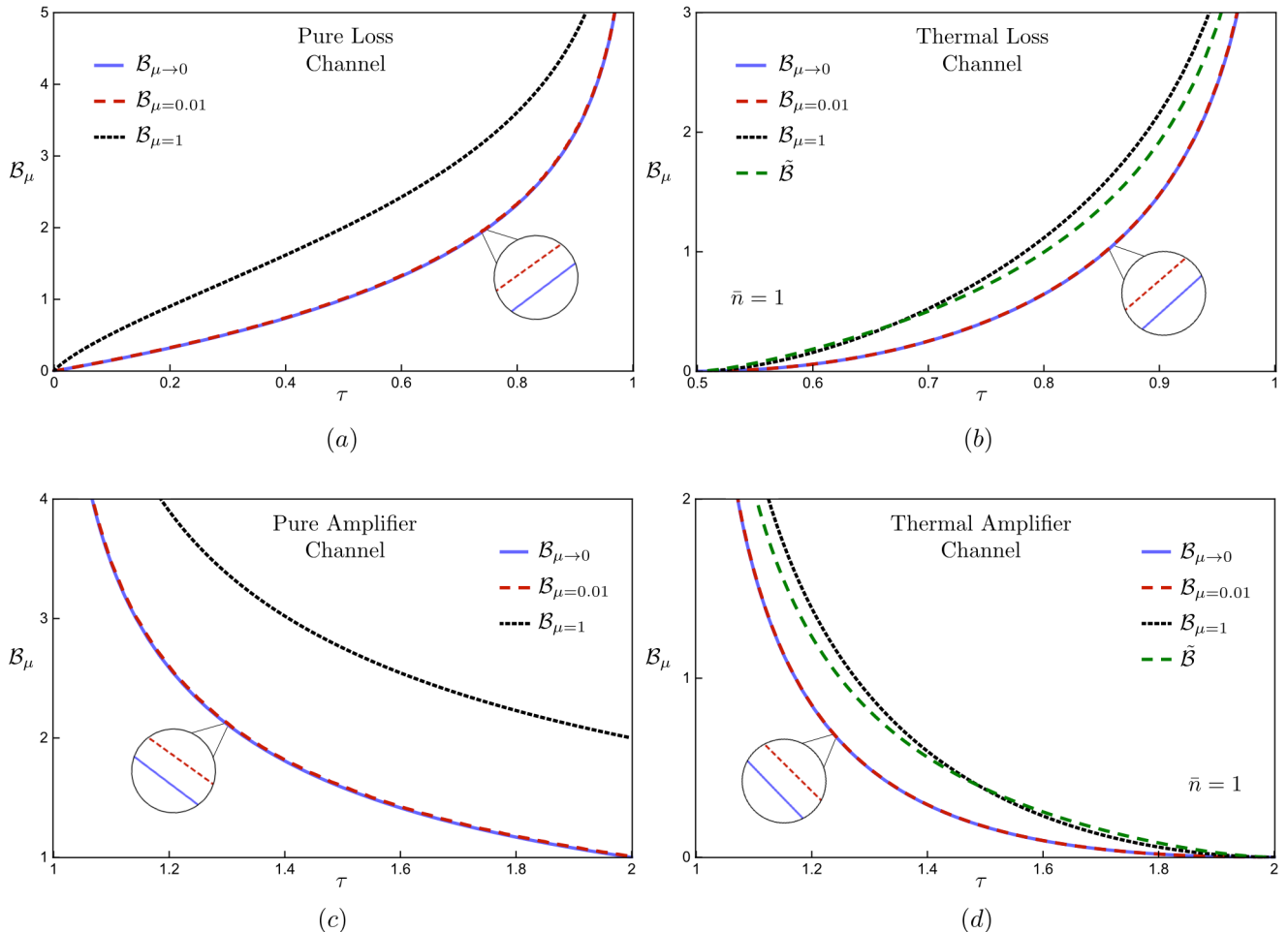


FIG. 3. Upper bounds to the secret-key rate capacity of lossy and amplifier channels (secret bits per channel use versus transmissivity  $0 < \tau < 1$  or gain  $\tau > 1$ ). In panels (a) and (c) we show the results for pure loss and pure amplifier channels, while panels (b) and (d) show the corresponding results for thermal loss and thermal amplifier channels with  $\bar{n} = 1$ . In the panels the lower blue line indicates the infinite-energy bound  $\mathcal{B}_0$  of Ref. [27] while the green dashed line is the approximate finite-energy bound  $\tilde{\mathcal{B}}$  of Ref. [45], which is computed over the class of states of Ref. [42]. Then, we show our improved finite-energy bound  $\mathcal{B}_\mu$  which is plotted for purity  $\mu = 1$  (black dashed line) and  $\mu = 0.01$  (red dashed line). Note that for pure loss channels the previous bound given in [45] coincides with our finite-bound  $\mathcal{B}_{\mu=1}$ . As we see for decreasing values of purity we can approximate  $\mathcal{B}_0$  as closely as we wish, while keeping the energy of the resource state finite (although large).

### A. Thermal-loss channels

A thermal-loss channel  $\mathcal{L}$  can be modeled as a beam-splitter operation,  $\exp[\theta(\hat{a}^\dagger \hat{b} - \hat{a} \hat{b}^\dagger)]$ , with transmissivity  $\tau = \cos^2 \theta$ , which mixes the input state together with an environmental thermal state with variance  $2\bar{n} + 1$ . It is a pure-loss channel  $\mathcal{L}_p$  for  $\bar{n} = 0$ . As shown in Ref. [27], the secret-key capacity of the thermal-loss channel  $\mathcal{L}$  is upper bounded by

$$K(\mathcal{L}) \leq \mathcal{B}_0(\mathcal{L}) \quad (25)$$

$$= \begin{cases} -\log_2[(1-\tau)\tau^{\bar{n}}] - h(\bar{n}), & \text{for } \bar{n} < \frac{\tau}{1-\tau}, \\ 0, & \text{otherwise,} \end{cases}$$

where we set  $h(x) := (x+1)\log_2(x+1) - x\log_2 x$ . For the pure-loss channel  $\mathcal{L}_p$  we have the exact formula [27]

$$K(\mathcal{L}_p) = \mathcal{B}_0(\mathcal{L}_p) = -\log_2(1-\tau). \quad (26)$$

Let us now compute the finite-energy bound  $\mathcal{B}_\mu$  for the thermal-loss channel, by fixing the purity  $\mu$  of our resource states and optimizing over the remaining free parameter as in Eq. (23). In this case, we may then write the upper bound  $K(\mathcal{L}) \leq \mathcal{B}_0(\mathcal{L}) \leq \mathcal{B}_\mu(\mathcal{L})$ , for different values of  $\mu$ . As shown in Fig. 3, the finite energy bound  $\mathcal{B}_\mu$  rapidly approaches  $\mathcal{B}_0(\mathcal{L})$  for decreasing purity  $\mu$ . This finite-energy approximation can be made as close as required because of Eq. (24). In Fig. 3, we also show the performance of the finite-energy bound for the pure-loss channel, in which case the purity  $\mu$  is the only degree of freedom. In Appendix B, we provide a non-asymptotic study of our finite-energy bound.

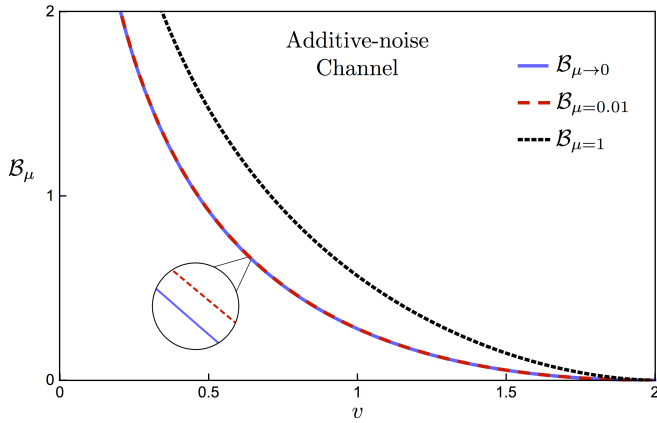


FIG. 4. Upper bounds to the secret-key capacity of the additive-noise Gaussian channel (secret bits per channel use versus added noise  $v$ ). The lower blue line indicates the infinite-energy bound  $\mathcal{B}_0$  of Ref. [27]. Then, we show our improved finite-energy bound  $\mathcal{B}_\mu$  which is plotted for purity  $\mu = 1$  (black dashed line) and  $\mu = 0.01$  (red dashed line). Note that the previous bound given in [45] coincides with our finite-bound  $\mathcal{B}_{\mu=1}$ . As we see for decreasing values of purity we can approximate  $\mathcal{B}_0$  as closely as we wish, while keeping the energy of the resource state finite (despite being large).

### B. Quantum amplifiers

A quantum amplifier channel  $\mathcal{A}$  can be modeled by a two-mode squeezing operation  $\exp[r(\hat{a}\hat{b} - \hat{a}^\dagger\hat{b}^\dagger)/2]$  with gain  $\tau = \cosh 2r$ , where  $r$  is the squeezing parameter [64], which is applied to the input state together with an environmental thermal state with  $\bar{n}$  mean photons. In general, for a thermal amplifier  $\mathcal{A}$ , we may write the following infinite-energy bound [27]

$$K(\mathcal{A}) \leq \mathcal{B}_0(\mathcal{A}) \quad (27)$$

$$= \begin{cases} -\log_2\left(\frac{\tau-1}{\tau\bar{n}+1}\right) - h(\bar{n}), & \text{for } \bar{n} < (\tau-1)^{-1}, \\ 0, & \text{otherwise.} \end{cases}$$

For  $\bar{n} = 0$ , we have a pure amplifier  $\mathcal{A}_p$  and its secret-key capacity is exactly known as [27]

$$K(\mathcal{A}_p) = \mathcal{B}_0(\mathcal{A}_p) = -\log_2(1 - \tau^{-1}). \quad (28)$$

By repeating the previous calculations, we may optimize over the class of Eqs. (13)-(15) at fixed purity  $\mu$ . In Fig. 3 we see that for decreasing  $\mu$ , we can approximate  $\mathcal{B}_0(\mathcal{A})$  and  $\mathcal{B}_0(\mathcal{A}_p)$  as closely as we wish.

### C. Additive-noise Gaussian channel

An additive-noise Gaussian channel  $\mathcal{N}$  is an asymptotic case of either loss or thermal channels where  $\tau \approx 1$  and a highly thermal state, i.e., classical, at the environmental input. It is known that its secret-key capacity is upper-bounded as follows [27]

$$K(\mathcal{N}) \leq \mathcal{B}_0(\mathcal{N}) \quad (29)$$

$$= \begin{cases} \frac{v-2}{2\ln 2} - \log_2(v/2), & \text{for } v < 2, \\ 0, & \text{otherwise.} \end{cases}$$

Here we assume the class specified by Eqs. (18)-(20) for decreasing values of purity. The corresponding finite-energy bound  $\mathcal{B}_\mu(\mathcal{N})$  well-approximates the infinite-energy bound  $\mathcal{B}_0(\mathcal{N})$ , as shown in Fig. 4.

## V. CONCLUSIONS

In this work, we have improved the finite-energy upper bounds to the secret-key capacities of one-mode phase-insensitive Gaussian channels. In particular, we have shown that our finite-energy bounds can be made as close as needed to the infinite-energy bounds of Ref. [27]. This is possible because we are employing the general class of resource states recently derived in Ref. [47]. This class perfectly simulates Gaussian channels while it simultaneously allows us to approach the asymptotic Choi matrix by decreasing purity. For this reason, we can always consider a perfect simulation with a finite-energy resource state which can be made sufficiently close to the optimal one (i.e., the asymptotic Choi matrix).

Such an approach removes the need for using an asymptotic simulation at the level of the resource state, even though the infinite energy limit still remains at the level of Alice's quantum measurement which is ideally a CV Bell detection (i.e., a projection onto displaced EPR states). Note that our study regards point-to-point communication, but it can be immediately extended to repeater chains and quantum networks [65, 66]. It would also be interesting to study the performance of the new class of resource states in the setting of adaptive quantum metrology and quantum channel discrimination [67, 68].

## ACKNOWLEDGEMENTS

This research has been supported by the Australian Research Council (ARC) under the Centre of Excellence for Quantum Computation and Communication Technology (CE170100012), the EPSRC via the ‘‘UK Quantum Communications Hub’’ (EP/M013472/1), and the European Commission via ‘Continuous Variable Quantum Communications’ (CiViQ, Project ID: 820466).

### Appendix A: Gaussian Relative Entropy and its Variance

In this appendix we provide a self-contained proof of both the quantum relative entropy between two arbitrary Gaussian states [27] and its variance [70], which was obtained using the techniques introduced in [27, 59]. Compared to the original derivations, the following proofs have the advantage of being both more compact and more general, as they can be applied

to different conventions available in the literature. Indeed, from bosonic creation and annihilation operators we may define the bosonic quadrature operators  $\hat{x}_j = (\hat{a}_j + \hat{a}_j^\dagger)/\sqrt{2\kappa}$  and  $\hat{p}_j = -i(\hat{a}_j - \hat{a}_j^\dagger)/\sqrt{2\kappa}$  with different normalizations  $\kappa$ , where the convention used in the main text is recovered for  $\kappa = 1/2$ , while the convention used in [27, 59, 70] is recovered with  $\kappa = 1$ . The quadrature operators can be grouped into a vector  $\hat{q} := (\hat{x}_1, \hat{p}_1, \dots, \hat{x}_n, \hat{p}_n)^T$  that satisfies the following commutation relations

$$[\hat{q}, \hat{q}^T] = \frac{i\Omega}{\kappa}. \quad (\text{A1})$$

We note that the operators  $\kappa\hat{q}_i\hat{q}_j$  satisfy the same algebraic properties as the operators defined for  $\kappa = 1$ . As such we can write any Gaussian state using the operator exponential form [59]

$$\hat{\rho}(\sigma, u) = \exp\left[-\frac{\kappa}{2}(\hat{q} - u)^T \mathbf{G}(\hat{q} - u)\right] / Z_\rho, \quad (\text{A2})$$

where  $u := \langle \hat{q} \rangle_{\hat{\rho}} \in \mathbb{R}^{2n}$  is the first moment,

$$Z_\rho = \det\left(\kappa\sigma + \frac{i\Omega}{2}\right)^{1/2}, \quad (\text{A3})$$

and the *Gibbs matrix*  $\mathbf{G}$  is related to the CM  $\sigma$  by

$$\mathbf{G} = 2i\Omega \coth^{-1}(2\kappa\sigma i\Omega), \quad \sigma = \frac{1}{2\kappa} \coth\left(\frac{i\Omega\mathbf{G}}{2}\right) i\Omega. \quad (\text{A4})$$

For calculating the relative entropy and its variance it is important to study the expectation values of a generic quadratic operator  $\hat{q}^T \mathbf{A} \hat{q}$ , where  $\mathbf{A}$  is a symmetric matrix. We focus here on states with zero displacement  $u = 0$ , as the generalization is straightforward. The product of two operators can be expressed as

$$\hat{q}_j \hat{q}_k = \hat{q}_j \circ \hat{q}_k + [\hat{q}_j, \hat{q}_k]/2 = \hat{q}_j \circ \hat{q}_k + \frac{i\Omega_{jk}}{2\kappa}, \quad (\text{A5})$$

where  $\hat{A} \circ \hat{B} = (\hat{A}\hat{B} + \hat{B}\hat{A})/2$ , and we have used the commutation relations of Eq. (A1). Since  $\Omega^T = -\Omega$ , for any symmetric  $\mathbf{A}$  we may write

$$\hat{q}^T \mathbf{A} \hat{q} = \frac{i}{2\kappa} \text{tr}[\mathbf{A}\Omega] + \sum_{jk} \hat{q}_j \circ \hat{q}_k A_{jk} \quad (\text{A6})$$

$$= \sum_{jk} \hat{q}_j \circ \hat{q}_k A_{jk}. \quad (\text{A7})$$

From the definition of the CM  $\sigma$  of a state  $\hat{\rho}$  we then find

$$\langle \hat{q}^T \mathbf{A} \hat{q} \rangle_{\hat{\rho}} = \text{tr}[\sigma \mathbf{A}]. \quad (\text{A8})$$

For calculating the variance of the operator  $\hat{q}^T \mathbf{A} \hat{q}$  we note that

$$\begin{aligned} \hat{q}^T \mathbf{A} \hat{q} \hat{q}^T \mathbf{A} \hat{q} &= (\hat{q}^T \mathbf{A} \hat{q}) \circ (\hat{q}^T \mathbf{A} \hat{q}) = \\ &= \sum_{ijkl} A_{ij} A_{kl} (\hat{q}_i \circ \hat{q}_j) \circ (\hat{q}_k \circ \hat{q}_l), \end{aligned} \quad (\text{A9})$$

where Eq. (A7) was used. In Ref. [71] it has been shown that

$$\begin{aligned} \text{tr}[\hat{\rho}(\hat{q}_i \circ \hat{q}_j) \circ (\hat{q}_k \circ \hat{q}_l)] &= \sigma_{ij}\sigma_{kl} + \sigma_{ik}\sigma_{jl} + \sigma_{il}\sigma_{jk} - \\ &\quad - \frac{1}{4\kappa^2} \Omega_{ik}\Omega_{jl} - \frac{1}{4\kappa^2} \Omega_{il}\Omega_{jk}. \end{aligned} \quad (\text{A10})$$

Combining the above expression with Eq. (A9) we find

$$\langle (\hat{q}^T \mathbf{A} \hat{q})^2 \rangle_{\hat{\rho}} = \text{tr}[\sigma \mathbf{A}]^2 + 2\text{tr}[\mathbf{A}\sigma \mathbf{A}\sigma] - \frac{1}{2\kappa^2} \text{tr}[\mathbf{A}\Omega \mathbf{A}\Omega^T], \quad (\text{A11})$$

and, in particular, the variance

$$\langle (\hat{q}^T \mathbf{A} \hat{q} - \langle \hat{q}^T \mathbf{A} \hat{q} \rangle_{\hat{\rho}})^2 \rangle_{\hat{\rho}} = 2\text{tr}[\mathbf{A}\sigma \mathbf{A}\sigma] + \frac{1}{2\kappa^2} \text{tr}[\mathbf{A}\Omega \mathbf{A}\Omega]. \quad (\text{A12})$$

We are now ready to show how to compute the relative entropy  $S(\hat{\rho}_1 \|\hat{\rho}_2)$  and its variance  $V(\hat{\rho}_1 \|\hat{\rho}_2)$ , defined as

$$S(\hat{\rho}_1 \|\hat{\rho}_2) = \text{tr}[\hat{\rho}_1 (\log_2 \hat{\rho}_1 - \log_2 \hat{\rho}_2)], \quad (\text{A13})$$

$$V(\hat{\rho}_1 \|\hat{\rho}_2) = \text{tr}\left[\hat{\rho}_1 \hat{\Delta}(\hat{\rho}_1, \hat{\rho}_2)^2\right], \quad (\text{A14})$$

where

$$\hat{\Delta}(\hat{\rho}_1, \hat{\rho}_2) = \log_2 \hat{\rho}_1 - \log_2 \hat{\rho}_2 - S(\hat{\rho}_1 \|\hat{\rho}_2). \quad (\text{A15})$$

Consider two generic Gaussian states  $\hat{\rho}_1 = \hat{\rho}(\sigma_1, u_1)$  and  $\hat{\rho}_2 = \hat{\rho}(\sigma_2, u_2)$ . Without loss of generality we may define the states  $\tilde{\rho}_1 = \hat{D}(u_1)^\dagger \hat{\rho}(\sigma_1, u_1) \hat{D}(u_1) = \hat{\rho}(\sigma_1, 0)$  and  $\tilde{\rho}_2 = \hat{D}(u_1)^\dagger \hat{\rho}(\sigma_2, u_2) \hat{D}(u_1) = \hat{\rho}(\sigma_2, \delta)$ , with  $\delta = u_2 - u_1$ , and where  $\hat{D}(u)$  is the displacement operator [8]. Indeed, due to unitary invariance  $S(\hat{\rho}_1 \|\hat{\rho}_2) = S(\tilde{\rho}_1 \|\tilde{\rho}_2)$  and  $V(\hat{\rho}_1 \|\hat{\rho}_2) = V(\tilde{\rho}_1 \|\tilde{\rho}_2)$ . From the exponential form of Eq. (A2) we find

$$-\log_2 \tilde{\rho}_1 = \frac{2 \ln Z_{\rho_1} + \kappa \hat{q}^T \mathbf{G}_1 \hat{q}}{2 \ln 2}, \quad (\text{A16})$$

$$-\log_2 \tilde{\rho}_2 = \frac{2 \ln Z_{\rho_2} + \kappa (\hat{q} - \delta)^T \mathbf{G}_2 (\hat{q} - \delta)}{2 \ln 2}, \quad (\text{A17})$$

so the relative entropy is obtained by taking the expectation value of the above operators over  $\tilde{\rho}_1 \equiv \rho(\sigma_1, 0)$ . Therefore, from Eqs. (A3) and (A8), and since  $\langle \hat{q}_j \rangle_{\tilde{\rho}_1} = 0$ , we may compute the entropic functional

$$\Sigma(\sigma_1, \sigma_j, \delta) := -\text{tr}(\tilde{\rho}_1 \log_2 \tilde{\rho}_j) = \quad (\text{A18})$$

$$= \frac{\ln \det\left(\kappa\sigma_j + \frac{i\Omega}{2}\right) + \kappa \text{tr}(\sigma_1 \mathbf{G}_j) + \kappa \delta^T \mathbf{G}_j \delta}{2 \ln 2}, \quad (\text{A19})$$

from which we obtain the relative entropy (A13) as

$$S(\hat{\rho}_1 \|\hat{\rho}_2) = -\Sigma(\sigma_1, \sigma_1, 0) + \Sigma(\sigma_1, \sigma_2, \delta). \quad (\text{A20})$$

The computation of the relative entropy variance is straightforward. In fact we note that, from the exponential form in Eq. (A2) and the relative entropy in Eqs. (A19)-(A20), we may write

$$\begin{aligned} \hat{\Delta} &= \log_2 \tilde{\rho}_1 - \log_2 \tilde{\rho}_2 - S(\tilde{\rho}_1 \| \tilde{\rho}_2) = \\ &= \log_2 Z_2 - \log_2 Z_1 + \frac{\kappa(\hat{q} - \delta)^T \mathbf{G}_2 (\hat{q} - \delta)}{2 \ln 2} - \frac{\kappa \hat{q}^T \mathbf{G}_1 \hat{q}}{2 \ln 2} \\ &\quad + \log_2 Z_1 - \log_2 Z_2 - \frac{\kappa \text{Tr}[\boldsymbol{\sigma}_1 (\mathbf{G}_2 - \mathbf{G}_1)]}{2 \ln 2} - \frac{\kappa \delta^T \mathbf{G}_2 \delta}{2 \ln 2} \\ &= \frac{\hat{q}^T (\mathbf{G}_2 - \mathbf{G}_1) \hat{q} - \text{tr}[\boldsymbol{\sigma}_1 (\mathbf{G}_2 - \mathbf{G}_1)] - 2\delta^T \mathbf{G}_2 \delta}{2\kappa^{-1} \ln 2}, \end{aligned} \quad (\text{A21})$$

where  $\text{tr}[\boldsymbol{\sigma}_1 (\mathbf{G}_2 - \mathbf{G}_1)] = \langle \hat{q}^T (\mathbf{G}_2 - \mathbf{G}_1) \hat{q} \rangle_{\tilde{\rho}_1}$ . Since  $\tilde{\rho}_1$  is a Gaussian state with zero first moment, the expectation value of odd products of  $\hat{q}$  is zero. Therefore, the relative entropy variance is obtained from the variance of  $\hat{q}^T (\mathbf{G}_2 - \mathbf{G}_1) \hat{q}$ , plus a correction due to the displacement  $\delta$ . From Eqs. (A12) and (A8) the final result is then

$$V(\hat{\rho}_1 \| \hat{\rho}_2) = \frac{4\kappa^2 \text{tr}[\boldsymbol{\sigma}_1 \tilde{\mathbf{G}} \boldsymbol{\sigma}_1 \tilde{\mathbf{G}}] + \text{tr}[\tilde{\mathbf{G}} \boldsymbol{\Omega} \tilde{\mathbf{G}} \boldsymbol{\Omega}] + \delta^T \mathbf{B} \delta}{2(2 \ln 2)^2}, \quad (\text{A22})$$

where  $\tilde{\mathbf{G}} = \mathbf{G}_1 - \mathbf{G}_2$ ,  $\delta = u_1 - u_2$  and  $\mathbf{B} = 8\kappa^2 \mathbf{G}_2 \boldsymbol{\sigma}_1 \mathbf{G}_2$ .

## Appendix B: Non-asymptotic behaviour

Consider an adaptive  $(n, \epsilon)$ -protocol of key generation, meaning that Alice and Bob use  $n$  times the channel to achieve a target state which is  $\epsilon$ -close to a private state with  $R_{n,\epsilon}$  secret bits. In particular, assume that the channel is a thermal-loss channel  $\mathcal{L}$  with transmissivity  $\tau$  and noise  $v = 2\bar{n} + 1$ . We can then simulate the channel by teleporting over our resource state  $\hat{\rho}_{\tau,v}$ ; next we may apply teleportation stretching to the adaptive protocol, and compute the REE on its simplified output in order to get a single-letter upper bound to the  $n$ -use  $\epsilon$ -secure secret-key capacity of the channel  $K_{n,\epsilon}(\mathcal{L})$ .

Building on this recipe designed in Ref. [27], one may write the following expansion in  $n$

$$\begin{aligned} K_{n,\epsilon}(\mathcal{L}) &\leq \Phi_n(\tau, v, \epsilon, \mu) \\ &:= \mathcal{B}_\mu + \sqrt{n^{-1} V(\hat{\rho}'_{\tau,v})} F(\epsilon) + O\left(\frac{\log n}{n}\right), \end{aligned} \quad (\text{B1})$$

where  $\mathcal{B}_\mu$  is the asymptotic finite-energy bound for fixed purity  $\mu$  computed over an optimal resource state  $\hat{\rho}'_{\tau,v}$ ,  $V(\hat{\rho}'_{\tau,v})$  is its relative entropy variance (A14), where  $V(\hat{\rho}) := V(\hat{\rho} \| \hat{\rho}_{\text{sep}}^*)$ , and  $F$  is the inverse of the cumulative Gaussian distribution, namely

$$F(\epsilon) = \sup\{a \in \mathbb{R} \mid f(a) \leq \epsilon\}, \quad (\text{B2})$$

$$f(a) = (2\pi)^{-1/2} \int_{-\infty}^a dx \exp(-x^2/2). \quad (\text{B3})$$

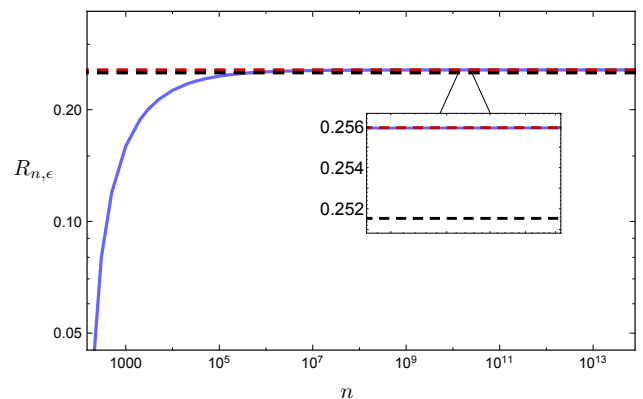


FIG. B1. Upper bound to the  $n$ -use  $\epsilon$ -secure secret-key capacity of the thermal-loss channel with  $\tau = 0.7$  and  $\bar{n} = 1$ . We assume  $\epsilon = 10^{-10}$  and purity  $\mu = 10^{-4}$ . We see how  $\Phi_n(\tau, v, \epsilon, \mu)$  (blue solid curve) tends to the asymptotic value  $\mathcal{B}_\mu$  for large  $n$  (red dashed line), which is slightly above the infinite-energy bound  $\mathcal{B}_0$  of Ref. [27] (black dashed line).

In Fig. B1, we numerically plot the upper bound  $\Phi_n(\tau, v, \epsilon, \mu)$  versus  $n$  uses of a thermal-loss channel with transmissivity  $\tau = 0.7$  and mean thermal number  $\bar{n} = 1$ , and assuming  $\epsilon = 10^{-10}$ . Our resource state is chosen with purity  $\mu = 10^{-4}$  and optimized over the remaining free parameter. The non-asymptotic bound is compared with the asymptotic bound  $\mathcal{B}_\mu$  and the infinite-energy bound  $\mathcal{B}_0$  of Ref. [27].

[1] J. Watrous, *The theory of quantum information* (Cambridge University Press, Cambridge, 2018).

[2] M. Hayashi, *Quantum Information Theory: Mathematical Foundation* (Springer-Verlag Berlin Heidelberg, 2017).

[3] M. A. Nielsen, and I. L. Chuang, *Quantum computation and quantum information* (Cambridge University Press, Cambridge, 2000).

[4] I. Bengtsson and K. Życzkowski, *Geometry of quantum states:*

- An Introduction to Quantum Entanglement* (Cambridge University Press, Cambridge 2006).
- [5] C. H. Bennett, and G. Brassard, Proc. IEEE International Conf. on Computers, Systems, and Signal Processing, Bangalore, pp. 175-179 (1984).
- [6] A. K. Ekert, Phys. Rev. Lett. **67**, 661-663 (1991).
- [7] N. Gisin, G. Ribordy, W. Tittel, and H. Zbinden, Rev. Mod. Phys. **74**, 145-196 (2002).
- [8] C. Weedbrook, S. Pirandola, R. García-Patrón, N. J. Cerf, T. C. Ralph, J. H. Shapiro, and S. Lloyd, Rev. Mod. Phys. **84**, 621-699 (2012).
- [9] G. Adesso, S. Ragy, and A. R. Lee, Open Syst. Inf. Dyn. **21**, 1440001 (2014).
- [10] S. L. Braunstein, and P. Van Loock, Rev. Mod. Phys. **77**, 513 (2005).
- [11] A. Serafini, *Quantum Continuous Variables: A Primer of Theoretical Methods* (CRC Press, 2017).
- [12] U. L. Andersen, J. S. Neergaard-Nielsen, P. van Loock, and A. Furusawa, Nat. Phys. **11**, 713-719 (2015)
- [13] S. Pirandola, S. L. Braunstein, and S. Lloyd, Phys. Rev. Lett. **101**, 200504 (2008).
- [14] F. Grosshans, G. Van Ache, J. Wenger, R. Brouri, N. J. Cerf, and P. Grangier, Nature (London) **421**, 238-241 (2003).
- [15] C. Weedbrook, A. M. Lance, W. P. Bowen, T. Symul, T. C. Ralph, and P. K. Lam, Phys. Rev. Lett. **93**, 170504 (2004).
- [16] S. Pirandola, S. Mancini, S. Lloyd, and S. L. Braunstein, Nat. Phys. **4**, 726 (2008).
- [17] V. C. Usenko and R. Filip, Phys. Rev. A **81**, 022318 (2010).
- [18] L. S. Madsen, V. C. Usenko, M. Lassen, R. Filip, and U. Andersen, Nat. Comm. **3**, 1083 (2012).
- [19] S. Pirandola *et al.*, Nat. Photon. **9**, 397 (2015).
- [20] E. Diamanti and A. Leverrier, Entropy **17**, 6072-6092 (2015).
- [21] V. C. Usenko, and F. Grosshans, Phys. Rev. A **92**, 062337 (2015).
- [22] V. C. Usenko and R. Filip, Entropy **18**, (2016).
- [23] S. Pirandola, R. García-Patrón, S. L. Braunstein, and S. Lloyd, Phys. Rev. Lett. **102**, 050503 (2009).
- [24] R. García-Patrón, S. Pirandola, S. Lloyd, and J. H. Shapiro, Phys. Rev. Lett. **102**, 210501 (2009).
- [25] I. Devetak, M. Junge, C. King, M. B. Ruskai, Comm. Math. Phys. **266**, 37 (2006).
- [26] M. Takeoka, S. Guha, and M. M. Wilde, Nat. Commun. **5**, 5235 (2014).
- [27] S. Pirandola, R. Laurenza, C. Ottaviani and L. Banchi, Nat. Comm. **8**, 15043 (2017).
- [28] V. Vedral, The role of relative entropy in quantum information theory. Rev. Mod. Phys. **74**, 197-234 (2002).
- [29] V. Vedral, M. B. Plenio, M. A. Rippin, and P. L. Knight, Phys. Rev. Lett. **78**, 2275 (1997).
- [30] C.H. Bennett, G. Brassard, C. Crepeau, R. Jozsa, A. Peres, and W. K. Wootters, Phys. Rev. Lett. **70**, 1895 (1993).
- [31] C. H., Bennett, D. P., DiVincenzo, J. A. Smolin and W. K. Wootters, Phys. Rev. A **54**, 3824-3851 (1996).
- [32] G. Bowen and S. Bose, Phys. Rev. Lett. **87**, 267901 (2001).
- [33] L. Vaidman, Phys. Rev. A **49**, 1473 (1994).
- [34] S. L. Braunstein and H. J. Kimble, Phys. Rev. Lett. **80**, 869 (1998).
- [35] T. C. Ralph, Opt. Lett. **24**, 348 (1999).
- [36] T. C. Ralph, P. K. Lam and R. E. S. Polkinghorne, J. Opt. B: Quantum Semiclass. Opt. **1**, 483-489 (1999).
- [37] S. L. Braunstein, G. M. D'Ariano, G. J., Milburn, and M. F. Sacchi, Phys. Rev. Lett. **84**, 3486-3489 (2000).
- [38] S. Pirandola *et al.*, Nat. Photon. **9**, 641-652 (2015).
- [39] G. Giedke and J.I. Cirac, Phys. Rev. A **66**, 032316 (2002).
- [40] J. Niset, J. Fiurášek, and N. J. Cerf, Phys. Rev. A **66**, 032316 (2002).
- [41] S. Pirandola, S. L. Braunstein, R. Laurenza, C. Ottaviani, T. P. W. Cope, G. Spedalieri and L. Banchi, Quantum Sci. Technol. **3**, 035009 (2018).
- [42] P. Liuzzo-Scorpo, A. Mari, V. Giovannetti and G. Adesso, Phys. Rev. Lett. **119**, 120503 (2017).
- [43] P. Liuzzo-Scorpo, A. Mari, V. Giovannetti and G. Adesso, Phys. Rev. Lett. **120**, 029904(E) (2018)
- [44] P. Liuzzo-Scorpo and G. Adesso, Proc. SPIE **10358**, Quantum Photonic Devices, 103580V (2017).
- [45] R. Laurenza, S. L. Braunstein, S. Pirandola, Sci. Rep. **8**, 15267 (2018).
- [46] E. Kaur and M. M. Wilde, Phys. Rev. A, **96**, 062318 (2017).
- [47] S. Tserkis, J. Dias, and T. C. Ralph, Phys. Rev. A **98**, 052335 (2018).
- [48] R. Simon, Phys. Rev. Lett. **84**, 2726 (2000).
- [49] L.-M. Duan, G. Giedke, J. I. Cirac and P. Zoller, Phys. Rev. Lett. **84**, 2722 (2000).
- [50] A. Serafini, F. Illuminati, and S. De Siena, J. Phys. B **37**, L21 (2004).
- [51] A. S. Holevo, Probl. Inf. Transm. **43**, 1 (2007).
- [52] F. Caruso, and V. Giovannetti, Phys. Rev. A **74**, 062307 (2006).
- [53] F. Caruso, V. Giovannetti, and A. S. Holevo, New J. Phys. **8**, 310 (2006).
- [54] Note that with the “hat” symbol, e.g.  $\hat{\rho}$ , we indicate density matrices while with bold  $\rho$  we indicate the corresponding covariance matrices.
- [55] G. Vidal and R. F. Werner, Phys. Rev. A **65**, 032314 (2002).
- [56] M. B. Plenio & S. S. Virmani *Quantum Information and Coherence, Ch. 8* (Springer, Switzerland, 2014).
- [57] R. Horodecki, P. Horodecki, M. Horodecki & K. Horodecki, Rev. Mod. Phys. **81**, 865-942 (2009).
- [58] G. Adesso, and F. Illuminati, J. Phys. A: Math. Theor. **40**, 7821-7880 (2007).
- [59] L. Banchi, S. L. Braunstein, and S. Pirandola, Phys. Rev. Lett. **115**, 260501 (2015)
- [60] Note that, more precisely, one should write  $\lim_{\omega} \Lambda_{\omega}(\hat{\sigma} \otimes \hat{\rho}_{\omega}^{\text{Choi}})$ , where  $\Lambda_{\omega}$  corresponds to a sequence of LOCCs, defined over a finite-energy implementation of the ideal CV Bell detection [27, 41].
- [61] Note that another solution is given by replacing  $\gamma$  with  $-\gamma$  in Eqs. (13)-(15). Also note that, for a specific choice of the symplectic eigenvalues, we recover the resource states of Ref. [42].
- [62] Note that states with reversed symmetry for each case, i.e.,  $a \leq b$  for  $\tau < 1$  and  $a \geq b$  for  $\tau > 1$ , can be retrieved by interchanging  $\nu_{-}$  and  $\nu_{+}$ , but then the corresponding range is given by  $1 \leq \nu_{\pm} \leq 2\bar{n} + 1$ .
- [63] K. Horodecki, M. Horodecki, P. Horodecki, and J. Oppenheim, Phys. Rev. Lett. **94**, 160502 (2005).
- [64] C. M. Caves, Phys. Rev. D **26**, 1817 (1982).
- [65] S. Pirandola, *Capacities of repeater-assisted quantum communications*, arXiv:1601.00966 (5 Jan 2016).
- [66] R. Laurenza, and S. Pirandola, Phys. Rev. A **96**, 032318 (2017).
- [67] S. Pirandola, and C. Lupo, Phys. Rev. Lett. **118**, 100502 (2017).
- [68] R. Laurenza, C. Lupo, G. Spedalieri, S. L. Braunstein, and S. Pirandola, Quantum Meas. Quantum Metrol. **5**, 1-12 (2018).
- [69] K. Li, Annals of Statistics **42**, 171-189 (2014).
- [70] M. M. Wilde, M. Tomamichel, S. Lloyd, M. Berta, Phys. Rev. Lett. **119**, 120501 (2017).
- [71] A. Monras and F. Illuminati, Physical Review A **81**, 062326 (2010).